NEOPLASIA
www.neoplasia.com

Volume 11 Number 12 December 2009 pp. 1292–1300 **1292**

Co-overexpression of Met and Hepatocyte Growth Factor Promotes Systemic Metastasis in NCI-H460 Non–Small Cell Lung Carcinoma Cells[1,2]

Roya Navab*,[3], Jiang Liu*,[3], Isolde Seiden-Long*,†,[3], Warren Shih*,‡, Ming Li*, Bizhan Bandarchi*, Yan Chen§, Davina Lau*, Yen-Fen Zu¶, Dave Cescon*, Chang Qi Zhu*, Shawna Organ*,‡, Emin Ibrahimov*, Dina Ohanessian* and Ming-Sound Tsao*,†,‡

*Ontario Cancer Institute and Princess Margaret Hospital, University Health Network, Toronto, Ontario, Canada M5G 2M9; †Medical Biophysics, University of Toronto, Toronto, Ontario, Canada; ‡Laboratory Medicine and Pathobiology, University of Toronto, Toronto, Ontario, Canada; §Tumor Institute, the Third Affiliated Hospital of Kunming Medical College, Kunming 650118, China; ¶Department of Oncology, 2nd People Hospital of Yunnan Province, Kunming, Yunnan, China, 650021

Abstract

Complete resection of early-stage non–small cell lung cancer (NSCLC) is potentially curative, yet approximately 50% of patients are at risk for developing metastatic recurrence. Met, the receptor for hepatocyte growth factor (HGF) is a receptor tyrosine kinase with demonstrated roles in regulating cellular proliferation, motility, morphogenesis, and apoptosis. Met receptor and its ligand, HGF, are commonly overexpressed in NSCLC, and their overexpression has been associated with poor prognosis, which could potentially involve a paracrine and/or autocrine activation loop. However, there is as yet no direct evidence that HGF-Met signaling directly promotes metastasis in NSCLC cells. Using retroviral transduction, we overexpressed the human *c-met* and *hgf* complementary DNA, alone or in combination in the NCI-H460 human large cell carcinoma cell line. The HGF/Met co-overexpressing (H460-HGF/Met) cells demonstrated enhanced tumorigenicity in xenograft *SCID* mice. When these cells are implanted orthotopically into the lungs of nude rats, only the H460-HGF/Met cells showed higher spontaneous metastases to distant organs including bone, brain, and kidney. These results provide evidence that autocrine overactivation of the Met-HGF loop enhances systemic metastases in NSCLC. Targeted interference of this loop may potentially be an effective adjuvant therapy to improve survival of early-stage NSCLC patients.

Neoplasia (2009) 11, 1292–1300

Abbreviations: HGF, hepatocyte growth factor; GFP, green fluorescent protein; Met, hepatocyte growth factor receptor; MMP-2, matrix metalloproteinase-2; MMP-9, matrix metalloproteinase-9; NSCLC, non–small cell lung cancer; SCID mice, severe combine immunodeficient mice; VEGF, vascular endothelial growth factor

Address all correspondence to: Dr. Ming-Sound Tsao, Room 7-613, Princess Margaret Hospital, 610 University Ave, Toronto, Ontario, Canada M5G 2M9.
E-mail: Ming.Tsao@uhn.on.ca

[1]This study was supported by Canadian Institutes of Health Research grant MOP-64345.
[2]This article refers to supplementary materials, which are designated by Figures W1 to W5 and are available online at www.neoplasia.com.
[3]Drs. Navab, Liu and Seiden-Long contributed equally to this work.
Received 14 April 2009; Revised 29 August 2009; Accepted 1 September 2009

DOI 10.1593/neo.09622

Introduction

Lung cancer is the leading cause of cancer-related death in North America and worldwide [1–3]. The 5-year survival rate of lung carcinoma has remained relatively unchanged at 15% for the past two decades. Non–small cell lung cancer (NSCLC) comprises approximately 80% of all lung cancers, and early-stage NSCLCs are potentially curative by complete surgical resection. However, even with surgical resection, the overall 5-year survival rate for these patients is 45% to 70%, with most deaths being due to metastatic recurrence. The factors that are responsible for early metastasis in NSCLC remain unknown. Deregulated overexpression of receptor tyrosine kinases has been reported to promote tumor cell motility and invasion and has been associated with poor prognosis.

The hepatocyte growth factor (HGF) receptor Met is a receptor tyrosine kinase that plays an important role in regulating cellular proliferation, motility, morphogenesis, and apoptosis [1]. The *c-met* gene was originally identified as a cellular counterpart of the chemically induced oncogene *tpr-met* isolated from a human osteosarcoma cell line [4]. The *c-met* gene encodes a high-affinity receptor for HGF [5]. HGF binding activates the tyrosine kinase of Met receptor resulting in autophosphorylation of several tyrosine residues in its cytoplasmic domain [6,7]. The phosphorylation of each tyrosine residue initiates distinct signal transduction cascades involving Erk, Akt, and Stat3 [6,7]. The *c-Met* gene amplification and/or overexpression have been reported in a wide variety of cancer types including lung, stomach, liver, prostate, ovary, colon, and pancreatic cancers [8–13]. In lung adenocarcinoma, Met protein expression assessed by immunohistochemistry has been reported as an independent poor prognostic marker [14]. High serum and tumor tissue levels of HGF have also been reported to predict poor outcome in resected lung cancer patients [15,16]. The abrogation of Met signaling by ribozymes, small interfering RNA, and chemical inhibitors has been reported to suppress the invasion and metastasis of tumor cells [6,7]. Data suggest that the HGF-Met loop is one of the factors that may promote metastasis in early-stage lung cancer [6,7]. However, direct experimental data to support this have not been forthcoming. In this study, we evaluated the *in vitro* and *in vivo* effects of forced co-overexpression of Met and HGF in the NCI-H460 human large cell carcinoma cell line. Our results provide strong evidence that ligand-dependent constitutive activation of Met in lung cancer cells may promote systemic metastasis.

Materials and Methods

Animals and Cell Lines

Male nude (CR:NIH-RNU) rats (Charles River, Inc, Frederick Cancer Research Facility, Frederick, MD) were received at 4 weeks of age and acclimatized for 1 to 2 weeks before entering study protocols. Rats were housed in sterilized cages and fed autoclaved food and water *ad libitum*. Severe combine immunodeficient (*SCID*) mice were bred on site and obtained from the Ontario Cancer Institute (OCI; Toronto, Ontario, Canada) animal facility. All manipulations were done under sterile conditions in a laminar flow hood, in accordance with procedures approved by the Institutional Animal Care Committee at the OCI. The general health of the animals was assessed daily.

NCI-H460 and Phoenix 293T Ampho cell lines were obtained from the American Type Culture Collection (Rockville, MD). NCI-H460 cells were routinely cultured at 37°C in RPMI 1640 medium containing 5% fetal bovine serum (FBS). Phoenix 293T Ampho were routinely cultured in Dulbecco's modified Eagle medium supplemented with 10% FBS. Retropack PT67 cell line was obtained from Clontech (Mountain View, CA) and was routinely cultured in Dulbecco's modified Eagle medium supplemented with 10% FBS.

Phospho-Met (Tyr1234/1235, catalog no. 3126 and 3077) antibodies were purchased from Cell Signaling (Beverly, MA). Antibodies against human Met (C28), murine Met (B3), and HGF were obtained from Santa Cruz Biotech (Santa Cruz, CA). Human recombinant HGF and anti-hHGF were purchased from R&D Systems (Minneapolis, MN); human cytokeratin antibody, Cam 5.2 was from BD Company (Mississauga, Ontario, Canada), CONFIRM c-Met (SP44) rabbit monoclonal primary antibody was obtained from Ventana (Tucson, AZ).

c-Met Expression Constructs

The pBMN-Met and HGF construct was created by cloning the full-length human c-*Met* or *hgf* complementary DNA (cDNA) into the pBMN-IRES-GFP retroviral vector. The pBMN-IRES-GFP plasmid is part of the Phoenix Retroviral Packaging System (http://www.stanford.edu/group/nolan/plasmid_maps/pmaps.html). The dominant-negative *met* (dnMet) cDNA had three mutations (K1110A, Y1349F, and Y1356F) that eliminated phosphorylation at the kinase domain and the multifunctional docking site of the receptor. In addition, the 21–amino acid C-terminus of the human *met* cDNA has been replaced by 12 amino acids of murine *met* cDNA, allowing detection of this construct in human cells by immunoblot analysis for murine *Met* [17]. This dnMet cDNA was directionally cloned into the *Eco*RI and *Not*1 sites of pBMN-IRES-GFP. The *Eco*RI site was filled and destroyed during cloning. An additional HGF construct (pLXSN-HGF) was generously provided by Dr. Morag Park (McGill University).

Stable Met- and HGF-Overexpressing Cell Lines

To generate retrovirus, either the Phoenix 293T Amphotropic retroviral, or the Retropack PT67, packaging line was transfected with pBMN, pBMN-Met, pBMN-dnMet, pBMN-HGF or pLXSN-HGF constructs using Lipofectamine PLUS transfection reagent (Invitrogen, Burlington, Ontario, Canada). At 48 and 72 hours after transfection, retrovirus-containing medium was harvested, and cell debris was removed by centrifugation at 1500 rpm for 15 minutes. The H460 cells were transduced with viral supernatants in the presence of 8 μg/ml polybrene (Sigma Chemical, St Louis, MO) overnight. At 72 hours after transduction, the cells were trypsinized into single-cell suspension and sorted for high green fluorescent protein (GFP) expression by fluorescence-activated cell sorting. Sorting attained a 90% to 95% pure population of GFP expressing cells. Cell lines were monitored by flow cytometry for GFP expression for 10 passages. If any loss of GFP occurred, cells were resorted until the population stabilized (two sorts total). Stability of the line was monitored, and no loss of GFP expression occurred in 10 passages. For pLXSN-HGF transductants, cells were passaged 48 hours after transduction, and clones were selected with 0.8 mg/ml neomycin. The H460-HGF/Met cell line was generated by viral transduction of pLXSN-HGF to the H460-Met cells and selected by exposure to 0.8 mg/ml neomycin.

Messenger RNA Expression Assay

Total RNA (4 μg) was reverse-transcribed using Superscript II reverse transcriptase (Invitrogen). A 10-ng equivalent of complementary DNA was used for each quantitative polymerase chain reaction assay performed with the Stratagene Mx3000p Sequence Detection System using SYBR green 2× master mix (Stratagene, La Jolla, CA).

Intron-spanning primers for *HGF* and *Met* PCR amplification were designed using the Primer Express software (Perkin-Elmer Applied Biosystems, Foster City, CA). Primer sequences for human *HGF* quantification were (forward) 5′-CCGAGGCCATGGTGCTATAC-3′ and (reverse) 5′-TCCTTGACCTTGGATGCATTC-3′. For human *c-Met*, the primer sequences were (forward) 5′-ACCTTTGATATA-ACTGTTTACTTGTTGCA-3′ and (reverse) 5′-GCTTTAGGG-TGCCAGCATTTT-3′.

Western Blot Analysis

To extract total protein, cells and tumor tissues were homogenized in lysis buffer (1% Triton X-100, 10% glycerol, 50 mM HEPES, 150 mM NaCl, 1.5 mM $MgCl_2$, 10 mM sodium pyrophosphate, 100 mM NaF, 10 mM $Na_4P_2O_4$, 1 mM EDTA, 10 mg/ml aprotinin, 10 mg/ml leupeptin, 100 mg/ml phenylmethylsulfonyl fluoride, and 1 mM sodium orthovanadate), and the lysates were cleared by centrifugation. Protein samples were fractionated on SDS–polyacrylamide gel and transferred to polyvinyliden fluoride membranes. The membranes were blocked with Roche blocking reagent (Roche Diagnostics, Laval, Quebec, Canada). Primary antibodies were used in the following concentrations: hMet (100 ng/ml), mMet (200 ng/ml), pMet (Tyr1234/1235, catalog no.3126; 200 ng/ml), and HGF (200 ng/ml). After incubations with the appropriate secondary antibodies, immunoreactive protein bands were detected by enhanced chemiluminescence (Roche Diagnostics Canada). Equal protein loading was confirmed by reprobing the blot with antibody against reduced guanosine adenine dinucleotide phosphate.

Subcutaneous Tumorigenicity Assay

Animal studies followed protocols that have been approved by the institutional animal care committee. Two million cells were injected subcutaneously in the left shoulder region of 5-week-old male *SCID* mice (n = 8/cell line). Mice were examined every 2 days, and tumor length and width were measured using calipers. Tumor volume was calculated using the following formula (length × width^2)π / 6. At 17 days, mice were killed by CO_2 asphyxiation, and tumors were excised. Portions of tumors were snap-frozen and stored in liquid nitrogen or were fixed in 10% buffered formalin for routine histopathologic processing.

Orthotopic Model to Evaluate Metastatic Potential

Six groups of rats (n = 8/group) were randomly assigned for orthotopic implantation of various engineered H460 lines. The cell lines included H460-pBMN, H460-Met, H460-HGF, H460-dnMet, H460-HGF/Met clone 4-8, and H460-HGF/Met clone 4-9. When any animal from any group succumbed to the disease or demonstrated terminal sign and symptoms, a single animal from each of the other groups was killed. This allows a direct comparison of all groups at the same time point for tumor-associated end points, including primary tumor weight, mediastinal lymph node weight, and metastases. Survival was not an end point of the study. Animals that died less than 21 days after implantation were considered as postanesthetic or surgical-related complications and were excluded from the final comparative analysis.

The procedure for endobronchial tumor cell implantation in nude rats was previously reported in detail [18,19]. Before tumor implantation, animals received 5-Gy whole-body γ-radiation using the Gamma Cell 40 Exactor (Nordion International Inc, Ottawa, Ontario, Canada; 500 rad of whole-body γ radiation from a ^{127}Cs source and at 120 rad/min). Cultured tumor cells were harvested by trypsinization and adjusted to a final concentration of 1.5×10^6 cells/70 μl. Rats were anesthetized by intramuscular injection of ketamine/xylazine (110 and 12 mg/kg; CDMV, Inc, Guelph, Ontario, Canada) and endobronchially implanted with 1.5×10^6 cells using a 20-gauge, 1.88-inch-long Teflon catheter. The catheter was passed into the distal bronchus of right caudal lobe through a small tracheotomy incision. The cell suspension was injected. After withdrawal of the catheter, the tracheotomy was repaired with a 6-0 Proline suture (Ethicon, Inc, Sommerville, NJ), and the incision was closed with sterile wound clips. The rats were returned to their cages on sterile rolled drapes to maintain their semiupright position.

Assessment of Metastatic Potential

Animals were killed when they succumbed to the disease or death was pending because of tumor progression. Metastatic occurrences were assessed macroscopically and microscopically. Any visible tumor deposit other than the primary tumor was considered as metastasis. The internal organs including lung, kidney, brain, chest wall, and bone as well as mediastinal lymph nodes were removed from the killed animals. The specimens were weighed, fixed in 10% buffered formalin, serially sectioned, and processed for histologic examination. Portions of primary tumors were also harvested for snap freezing and storage in liquid nitrogen.

The primary tumor and lymph node weights, which reflect the tumor burden, were recorded. All tissues were serially sectioned and stained with hematoxylin and eosin for microscopic examination. Any macroscopic or microscopic tumor deposit discovered, other than the primary tumor, was considered a metastasis. Organs or tissues were counted as either positive or negative for metastasis. No assessment of number or extent of metastasis was made.

Immunohistochemistry

Formalin-fixed paraffin-embedded tissues were cut at 4-μm thickness and dried in 60°C oven overnight. Sections were dewaxed in xylene and rehydrated through graded alcohol to water. Endogenous peroxidase was blocked in 3% hydrogen peroxide. Heat-induced epitope retrieval was carried out in 10 mM citrate buffer, pH 6.0 in a Milestone T/T Mega microwave oven. After blocking for endogenous biotin with Vector's biotin blocking kit, sections were incubated in primary antibody (h-Met [SP44; Ventana, Tucson, AZ]; HGF [AF-294-NA, 1:300 dilution; R&D Systems]; phospho-Met [Tyr1234/1235, catalog no. 3077, 1:150 dilution; Cell Signaling]; mouse CD31 [sc-1506, 1:1000; Santa Cruz]) at room temperature in a moist chamber. After washing in PBS, slides were incubated in biotin-conjugated anti-goat IgG (HGF; Vector Laboratories, Burlingame, CA) or anti-rabbit IgG (h-Met and pMet) followed by streptavidin-HRP (ID Labs Inc, London, Canada) for 30 minutes each. Immunoreactivities were revealed by incubating in NovaRed substrate (Vector Laboratories) for 5 minutes. Slides were counterstained in Mayer's hematoxylin and mounted with Permount. Immunostaining for h-Met was performed using the Ventana's BenchMark XT System.

Assessment of Tumor Vascularity

Murine CD31 immunoperoxidase–stained sections were used to highlight the blood vessels. Blood vessels were counted based on a previously described method [20]. Any highlighted single endothelial cell or cell clusters were separately counted from the adjacent vessels. Vascular hot spots were selected on low magnification (100×), and the CD31-positive vessels/cells were counted in five fields (20× objective) at a magnification of ×200.

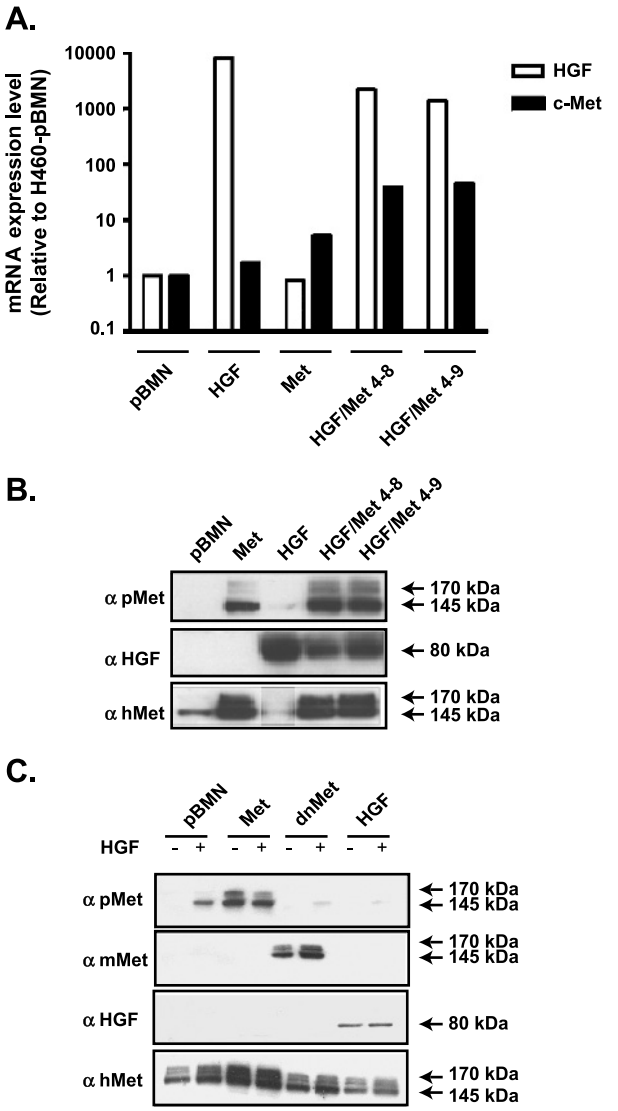

Figure 1. Establishment of stable HGF/Met expressing H460 cell lines. (A) The messenger RNA (mRNA) expression of human *hgf* and *c-met* in HGF-, Met-, and Met/HGF–overexpressing H460 cell lines were evaluated using RT-qPCR (data were expressed as relative level of mRNA expression compared with pBMN control). (B and C) Met and HGF H460 cell lines with or without HGF stimulation (20 ng/ml) were analyzed by Western blot for the activated receptor using phospho-Met–specific antibody (pMet—top panel) and the total Met receptor levels using human Met antibody (hMet—bottom panel). (C) dnMet-H460 cell line was used as a negative control. The accuracy of dnMet-H460 cell line was measured using antibody specific for mouse c-Met. No phosphorylation of c-Met was observed in dnMet-H460 cell line both in the absence and in the presence of HGF.

ELISA Assay for HGF and Vascular Endothelial Growth Factor Protein Levels

Using a DuoSet ELISA development system for human HGF and vascular endothelial growth factor (VEGF; R&D Systems). Ninety-six–well microplates (Nunc, Rochester, NY) were coated with 100 μl per well of mouse antihuman HGF and/or VEGF diluted in PBS overnight at 4°C. After blocking with 1% bovine serum albumin in PBS for 1 hour, plates were washed with PBS + 0.05% Tween 20 then 100 μl of tumor lysates or standards in PBS + 1% bovine serum albumin were added, and the plates were incubated for 2 hours at room temperature. After washing, biotinylated goat antihuman HGF and/or VEGF detection antibody was added for 2 hours at room temperature. After several washing steps, 100 μl of streptavidin-HRP was added to each well, and the plates were incubated for 20 minutes at room temperature. After washing, bound HGF and/or VEGF were revealed by reading absorbance at 450 nm. The assay was generally performed in duplicate.

Statistics

Two-way analysis of variance test was used to compare primary tumor weight and lymph node weight. Difference in tumor growth rates of xenografts was tested by using mixed-effects model estimation [21]. χ^2 and Fisher's exact test were used to compare the incidence of metastasis between each cell lines. Tests that produced $P \leq .05$ were considered

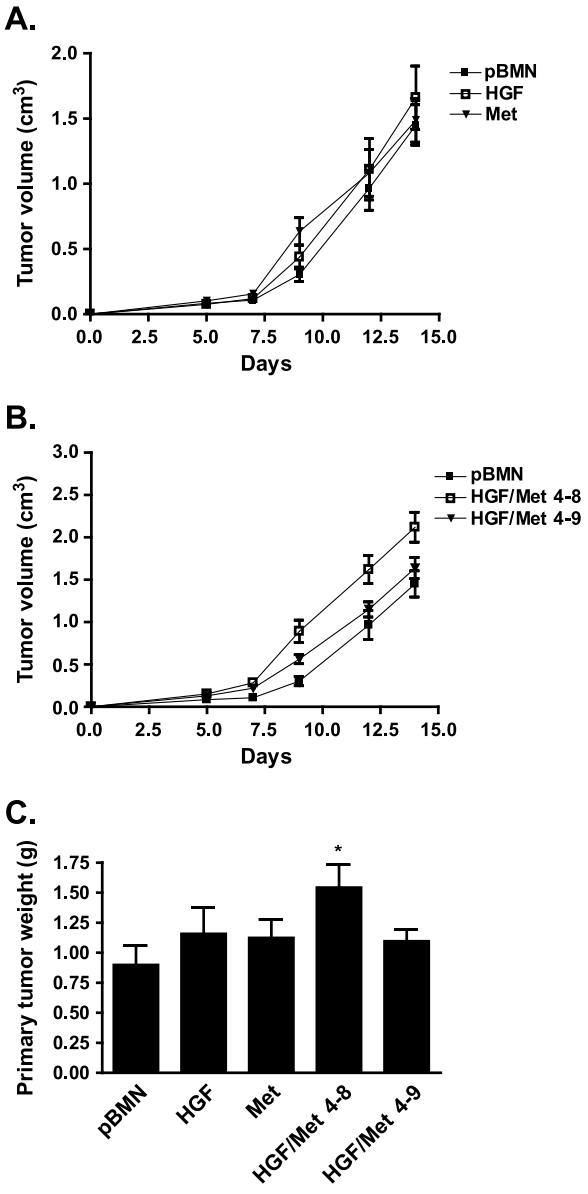

Figure 2. HGF/Met–overexpressing H460 tumor growth rate *in vivo*. (A and B) Experiment conducted in duplicate, and data are represented as mean ± SEM ($n = 8$). (C) Primary tumor weight.

to be significant. For the rest of other experiments, Mann-Whitney test was used.

Results

Establishment of H460 Met– and HGF-Overexpressing Cell Lines

Stable integration and expression of human Met receptor and HGF (hHGF) in H460 cells was monitored for more than 10 passages and confirmed by quantitative reverse transcription–PCR (RT-qPCR; Figure 1*A*) and Western blot analysis (Figure 1*B*). Expression of *c-met* but not *hgf* cDNA resulted in the HGF-independent constitutive activation of the receptor, as detected by Western blot with the antibody specific to phosphorylated $Y^{1234,1235}$Met (catalog no. 3126; Figure 1, *B* and *C*). Clones that overexpressed both Met and HGF (H460-HGF/Met 4-8 and 4-9) showed increased levels of phospho-Met compared with the H460-Met cell line (Figure 1*B*). Overexpression of HGF or HGF/Met did not alter the morphology of the cells (Figure W1), and they remained epithelial in appearances (Figures W2 and W3). HGF-overexpressing H460 cells showed compensatory down-regulation of Met protein level (Figure 1, *B* and *C*). The dnMet-H460 cell line suppressed the phosphorylation of the Met receptor even in the presence of the HGF ligand (Figure 1*C*).

Effect of Met and/or HGF Overexpression on Tumorigenicity of H460 Cells

When implanted subcutaneously in *SCID* mice, the H460-HGF and H460-Met cells showed growth rates similar to the H460-pBMN control cells (Figure 2*A*). In contrast, the H460-HGF/Met 4-8 and 4-9 clones showed increased growth rate compared with the H460-pBMN control cells (Figure 2*B*). The H460-HGF/Met 4-8 cells demonstrated increased growth rate ($P = .0034$) and tumor weight ($P = .0203$; Figure 2*C*). The expression of *c-met* and *hgf* in H460-tumor lines was verified by RT-qPCR (Figure 3, *A* and *B*). The increased constitutive activation of Met in tumors was also confirmed in H460-Met and both clones of H460-HGF/Met by Western blot analysis (Figure 3, *C* and *D*) and immunohistochemistry (Figure 4*A*) using phosphorylated Met specific antibody (Tyr1234/1235, catalog no. 3077). As a control, we showed that the dnMet-H460 tumor cells had markedly reduced Met

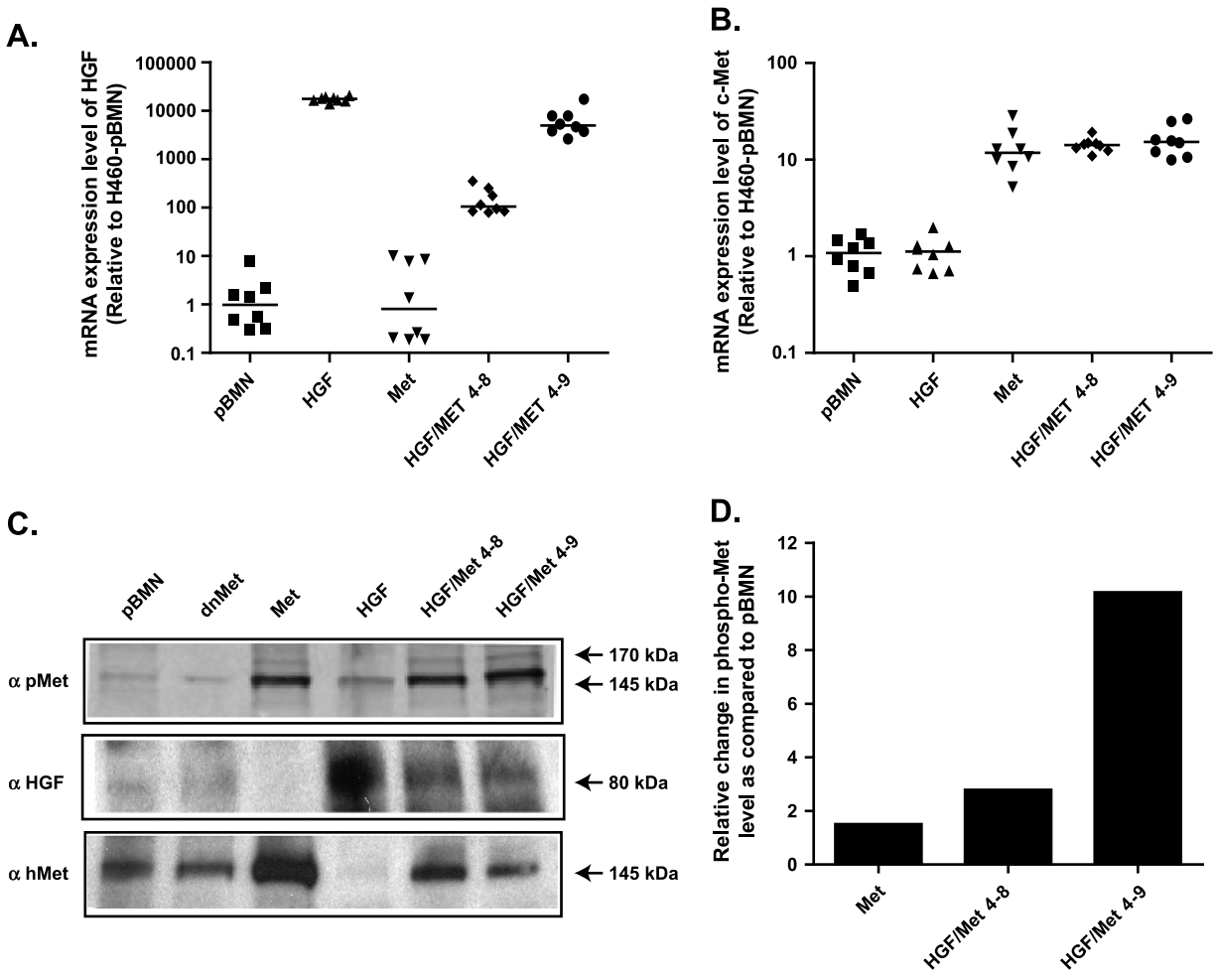

Figure 3. Expression of c-Met and hHGF in H460 tumors. (A and B) mRNA expression of human *hgf* and *c-met* was verified using RT-qPCR. (C) HGF and Met overexpression was detected in H460 tumors using Western blot for hHGF and c-Met and the activated Met receptor. H460-dnMet was used as a negative control. (D) Histogram shows the ratio between the two bands (phosphoprotein and total protein) relative to pBMN control. The intensity of the bands was measured using the microcomputer imaging device (MCID) program.

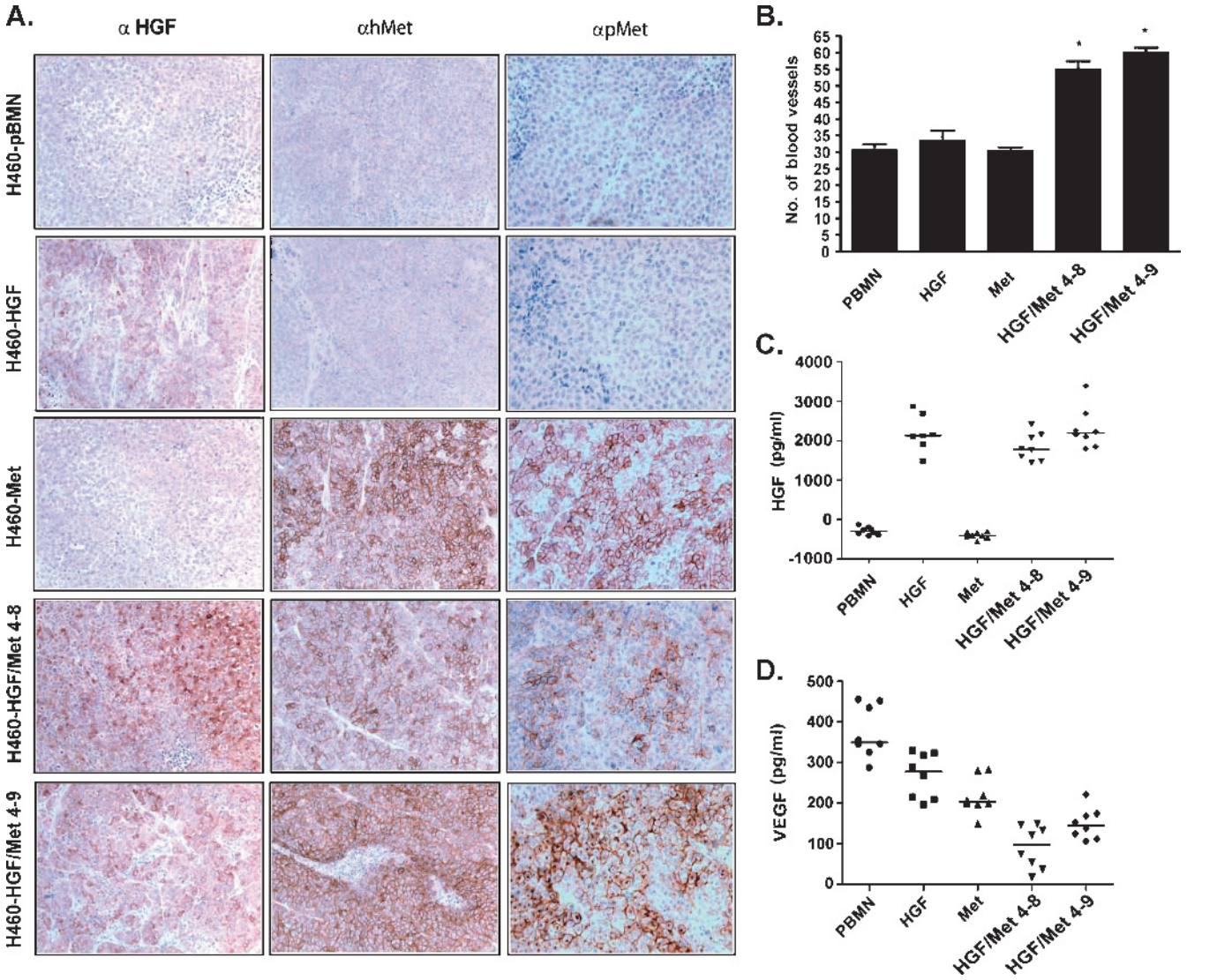

Figure 4. Constitutive activation of Met and HGF induced angiogenesis in HGF/Met–overexpressing H460 xenograft tumors. (A) Immunohistochemistry of xenografts formed by H460 cell lines without (pBMN) or with HGF and/or Met overexpression. (B) Number of mCD31-positive blood vessels in five fields of most vascular areas at 200× magnification. (C and D) Concentration of HGF and VEGF, respectively, in protein extracts of xenograft tumors by ELISA. Magnifications: ×100 for HGF; ×200 for h-Met and pMet. Asterisks (*) indicate statistical significance between groups.

receptor phosphorylation when compared with the Met-H460 tumor cells (Figure 3*C* and Figure W4).

HGF Enhances Angiogenesis in HGF/Met–Overexpressing Cells

Tumor angiogenesis was assessed by both qualitative method and intratumoral microvessel density assessment using staining with antimouse antibody to endothelial marker CD31 (mCD31). H460-HGF/Met 4-8 and 4-9 tumors showed higher intratumoral microvessel density than the control H460-pBMN (P = .008), H460-HGF, and H460-Met tumors (Figure 4*B*). Quantitative measurement of human HGF by ELISA showed the highest HGF content in H460-HGF, H460-HGF/Met 4-8, and 4-9 tumors compared with control H460-pBMN and H460-Met tumors (P = .0002; Figure 4*C*). In contrast, the VEGF contents of H460-HGF/Met tumors were lower than tumors formed by the other cell lines (Figure 4*D*), indicating that the increased vascularity in the former was most likely due to the overexpression of both Met and HGF.

HGF/Met Co-overexpression Enhanced Metastatic Potential of H460 Cells

Orthotopic implantation of lung cancer cells has been reported to mimic more the behavior of human lung cancer than the subcutaneous model [22]. Similar to the parental H460 line, H460-pBMN developed regional metastasis to mediastinal lymph nodes but very limited systemic metastases (1/7) to distant organs (Table 1). No significant differences were noted in the weight of the primary tumors formed by all cell lines. Both H460-Met and H460-HGF cells showed increased metastases to the bone, kidneys, and left lung but not to the brain and gum. Metastases to both the bone and kidneys appeared increased further in H460-HGF/Met cells (Table 1). Only the HGF/

Table 1. Effect of HGF/Met Expression on Metastases.

Cell Line	T wt (g), mean ± SD	LN wt (g), mean ± SD	Regional Mets No. Animals		Systemic Mets				No. Animals	
			LN	L. lung	Bone	Kidney	Brain	Gum	Systemic mets	Total No. animals
pBMN	4.6 ± 1.7	0.21 ± 0.21	7	2	0	1	1	0	1	7
HGF	4.1 ± 2.4	0.19 ± 0.27	8	7	4	2	1	1	4	8
Met	4.7 ± 3.1	0.36 ± 0.36	8	7	2	3	1	2	5	9
HGF/Met 4-8	4.4 ± 3.8	0.29 ± 0.22	8	7	4	6	1	2	7*	8
HGF/Met 4-9	4.9 ± 2.6	0.49 ± 0.47	7	7	6	7	4	4	8*	8

L. lung indicates left lung; *LN*, lymph node; *mets*, metastasis; *T*, primary tumor; *wt*, weight.
Incidence of systemic metastasis in orthotopic model using nude rat. The metastatic potential of lung cancer cell lines is demonstrated by their endobronchially orthotopic implantation of 1.5×10^6 cells/70 µl in the right caudal lobe. Animals were killed when they succumbed to the disease or death was pending owing to tumor progression. Metastatic occurrences were assessed macroscopically and microscopically. Any visible tumor deposit other than the primary tumor was considered as metastasis. Primary tumor weight and the weight of the mediastinal lymph node were measured to evaluate tumor burden.
*The H460-HGF/Met clones produced statistically significant systemic metastases (7/8 and 8/8, respectively) in the experimental animals when compared with the H460-pBMN cells ($P < .05$).

Met 4-9 cells that have the highest levels of Met and HGF coexpression showed increased metastases to the brain and gum. Overall, only the H460-HGF/Met clones produced statistically significant systemic metastases (7/8 and 8/8, respectively) in the experimental animals when compared with the H460-pBMN cells ($P < .05$; Table 1).

Using the HGF and Met antibody, tumors formed by the H460-HGF/Met 4-9 cells showed increased Met and HGF expression in both the primary and metastatic organ (lymph node) compared with pBMN control cells (Figure 5).

Discussion

We have demonstrated that overexpression of Met receptor with or without HGF co-overexpression in the H460 lung cancer cell line resulted in ligand-independent, constitutive activation of the receptor. In contrast, HGF overexpression alone did not. Whereas overexpression of either Met or HGF individually increased modestly the systemic metastasis of H460 cells, especially to bone and/or kidney, the co-overexpression of both the ligand and receptor further enhanced the metastatic potential of these cells. These results provide direct evidence that autocrine overactivation of the HGF-Met loop may promote systemic metastasis in NSCLC.

There is evidence that HGF and/or Met overexpression is associated with poor survival in NSCLC patients [11,14,23]. The coexpression of both HGF and Met has been detected in 50% to 52% of lung primary adenocarcinomas [13,14]. The HGF-Met system is currently thought to function mainly in a paracrine manner [24–26], with the tumor cells expressing the receptor and the ligand originating from the stromal fibroblasts. However, we have previously shown that HGF is expressed in primary NSCLC and by normal bronchial epithelial cells and many NSCLC cell lines that also demonstrated constitutive Met receptor autophosphorylation [27]. Autocrine HGF-Met signaling plays significant roles in the scattering activity, growth, and differentiation of human lung adenocarcinoma cells [28,29]. Autocrine

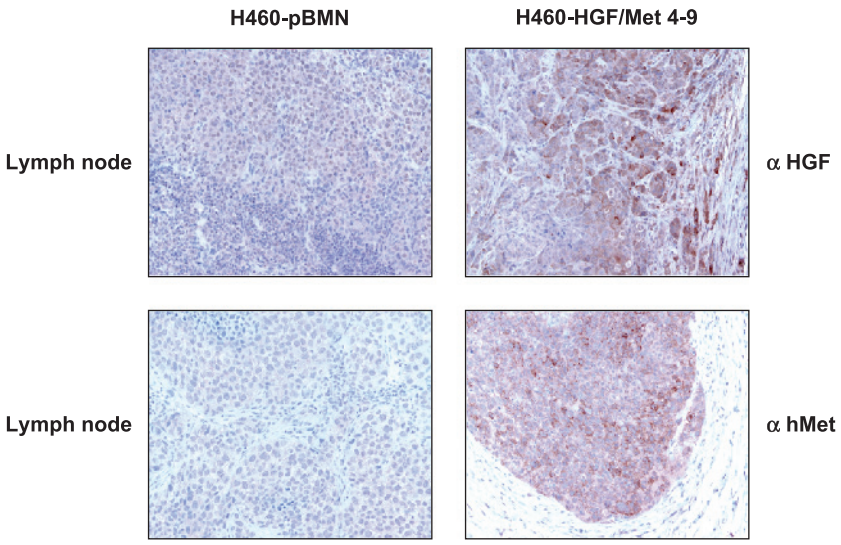

Figure 5. Metastatic potential of H460 cells implanted orthotopically is dependent on both HGF and Met expression. Immunohistochemistry evaluation of HGF and Met in lymph nodes of representative tissues from HGF/Met overexpressing H460 cell line clone 4-9 and control H460 cell line harboring empty vector (H460-pBMN).

Met-HGF expression has also been shown to be able to mediate tumorigenicity and metastasis in NIH 3T3 cells [30,31]. However, before the current study, it was unknown whether autocrine HGF-Met signaling was important in lung cancer metastasis.

Our laboratory has previously reported that the orthotopic implantation of H460 human lung carcinoma cell line could metastasize spontaneously to systemic organs [12,19], thus more accurately mimicking the progression of human lung cancer. The model involves two stages. First, the orthotopic implantation of H460 cells resulted in only mediastinal lymph node metastasis. Second, when the primary tumor was harvested and reimplanted into new hosts, systemic metastases to the bone, kidney, brain, and soft tissue such as gum were observed. Using this orthotopic model, the H460 overexpressing both Met and HGF resulted in spontaneous systemic metastasis without the two-stage process required for the parental H460 cells alone. However, only the H460-HGF/Met 4-9 cells demonstrated the highest spontaneous metastases to bone, kidney, brain, and gum. In contrast, the H460-HGF or -Met alone showed less metastases to all these sites. Interestingly, the H460-HGF/Met 4-8 cells also showed high metastatic rate to bone and kidney comparable to the 4-9 clone but demonstrated reduced metastases to brain and gum. Compared with the 4-9 clone, the H460-HGF/Met 4-8 cells showed a low level of Met autophosphorylation. This effect may arise from clonal variation leading to a reduced autocrine activity. This suggests that the HGF-Met autocrine loop plays a greater role in brain and gum metastases in this model. We have reported previously that an H460SM cell line selected for their spontaneous systemic metastasis ability similar to the H460-HGF/Met cells also showed increased expression of Met compared with the parental H460 cells, further supporting the importance of the HGF-Met loop in inducing systemic metastasis [32]. In this regard, we cannot rule out that Met overexpression alone may be sufficient to promote metastasis because mouse HGF does not react and activate human Met receptor [33].

We have also shown that the HGF/Met co-overexpressing cells form tumors with both increased vascularity and higher HGF tumor content. However, the H460 cells that overexpress HGF alone also highly express the VEGF yet did not show comparable metastatic potential. The finding indicates that increased vascularity and high HGF expression are not the only mechanism to increase metastasis. We previously reported that, in the NCI-H358 lung adenocarcinoma cells that have functionally active cell surface Met receptor, overexpression of HGF enhanced the cells' capacity to colonize soft agar and form subcutaneous xenograft tumors in *SCID* mice, without affecting the expression of VEGF [28]. Therefore, we postulate that the autocrine overactivation of the HGF-Met loop in NSCLC cells induces the expression of factors that further enhance angiogenesis, in addition to HGF and/or VEGF. Using gelatin zymography, we observed higher levels of both proactive and active forms (72 and 68 kDa, respectively) of MMP-2 and of MMP-9 (92 and 82 kDa, respectively) in the H460-HGF/Met tumors compared with control H460-pBMN (Figure W5). In this regard, we believe that the activity of MMP-2 and MMP-9 may also contribute to the enhanced angiogenesis and metastatic potential.

The necessity for coordinated activation of HGF and Met suggests that the tumor cells need to have co-overexpression of HGF and Met for their maximum effect on the promotion of metastasis. To our knowledge, there is no direct evidence stating that autocrine mechanism of HGF-Met signaling potentiates the metastasis of NSCLC cells. We believe that the orthotopic H460-HGF/Met models are good models to test Met or HGF inhibitors for their potential use in adjuvant therapy for lung cancer.

Acknowledgments

The authors thank Gary Nolan (Stanford University) for generously allowing the use of his pBMN retroviral transduction system for our studies, Trudey Nicklee for helping with the Microcomputer Imaging Device to measure the intensity of the bands in the Western blot analysis, and Morag Park for the HGF and c-Met constructs.

References

[1] Richardson GE and Johnson BE (1993). The biology of lung cancer. *Semin Oncol* **20**, 105–127.
[2] Kalemkerian GP (1994). Biology of lung cancer. *Curr Opin Oncol* **6**, 147–155.
[3] Gazdar AF (1990). Cell biology and molecular biology of small cell and non–small cell lung cancer. *Curr Opin Oncol* **2**, 321–327.
[4] Cooper CS, Park M, Blair DG, Tainsky MA, Huebner K, Croce CM, and Vande Woude GF (1984). Molecular cloning of a new transforming gene from a chemically transformed human cell line. *Nature* **311**, 29–33.
[5] Bottaro DP, Rubin JS, Faletto DL, Chan AM, Kmiecik TE, Vande Woude GF, and Aaronson SA (1991). Identification of the hepatocyte growth factor receptor as the *c-met* proto-oncogene product. *Science* **251**, 802–804.
[6] Ma PC, Maulik G, Christensen J, and Salgia R (2003). c-Met: structure, functions and potential for therapeutic inhibition. *Cancer Metastasis Rev* **22**, 309–325.
[7] Christensen JG, Burrows J, and Salgia R (2005). c-Met as a target for human cancer and characterization of inhibitors for therapeutic intervention. *Cancer Lett* **225**, 1–26.
[8] Nakamura Y, Niki T, Goto A, Morikawa T, Miyazawa K, Nakajima J, and Fukayama M (2007). c-Met activation in lung adenocarcinoma tissues: an immunohistochemical analysis. *Cancer Sci* **98**, 1006–1013.
[9] Kammula US, Kuntz EJ, Francone TD, Zeng Z, Shia J, Landmann RG, Paty PB, and Weiser MR (2007). Molecular co-expression of the *c-Met* oncogene and hepatocyte growth factor in primary colon cancer predicts tumor stage and clinical outcome. *Cancer Lett* **248**, 219–228.
[10] Bauer TW, Somcio RJ, Fan F, Liu W, Johnson M, Lesslie DP, Evans DB, Gallick GE, and Ellis LM (2006). Regulatory role of c-Met in insulin-like growth factor-I receptor–mediated migration and invasion of human pancreatic carcinoma cells. *Mol Cancer Ther* **5**, 1676–1682.
[11] Ichimura E, Maeshima A, Nakajima T, and Nakamura T (1996). Expression of c-met/HGF receptor in human non–small cell lung carcinomas *in vitro* and *in vivo* and its prognostic significance. *Jpn J Cancer Res* **87**, 1063–1069.
[12] Tsao MS, Liu N, Chen JR, Pappas J, Ho J, To C, Viallet J, Park M, and Zhu H (1998). Differential expression of Met/hepatocyte growth factor receptor in subtypes of non–small cell lung cancers. *Lung Cancer* **20**, 1–16.
[13] Masuya D, Huang C, Liu D, Nakashima T, Kameyama K, Haba R, Ueno M, and Yokomise H (2004). The tumour-stromal interaction between intratumoral c-Met and stromal hepatocyte growth factor associated with tumour growth and prognosis in non–small-cell lung cancer patients. *Br J Cancer* **90**, 1555–1562.
[14] Takanami I, Tanana F, Hashizume T, Kikuchi K, Yamamoto Y, Yamamoto T, and Kodaira S (1996). Hepatocyte growth factor and c-Met/hepatocyte growth factor receptor in pulmonary adenocarcinomas: an evaluation of their expression as prognostic markers. *Oncology* **53**, 392–397.
[15] Inoue T, Kataoka H, Goto K, Nagaike K, Igami K, Naka D, Kitamura N, and Miyazawa K (2004). Activation of c-Met (hepatocyte growth factor receptor) in human gastric cancer tissue. *Cancer Sci* **95**, 803–808.
[16] Ferracini R, Longati P, Naldini L, Vigna E, and Comoglio PM (1991). Identification of the major autophosphorylation site of the Met/hepatocyte growth factor receptor tyrosine kinase. *J Biol Chem* **266**, 19558–19564.
[17] Abdel-Ghany M, Cheng HC, Elble RC, and Pauli BU (2002). Focal adhesion kinase activated by β(4) integrin ligation to mCLCA1 mediates early metastatic growth. *J Biol Chem* **277**, 34391–34400.
[18] Wang KK, Liu N, Radulovich N, Wigle DA, Johnston MR, Shepherd FA, Minden MD, and Tsao MS (2002). Novel candidate tumor marker genes for lung adenocarcinoma. *Oncogene* **21**, 7598–7604.
[19] Howard RB, Mullen JB, Pagura ME, and Johnston MR (1999). Characterization of a highly metastatic, orthotopic lung cancer model in the nude rat. *Clin Exp Metastasis* **17**, 157–162.

[20] Weidner N, Semple JP, Welch WR, and Folkman J (1991). Tumor angiogenesis and metastasis—correlation in invasive breast carcinoma. *N Engl J Med* **324**, 1–8.

[21] Littell RC, Henry PR, and Ammerman CB (1998). Statistical analysis of repeated measures data using SAS procedures. *J Anim Sci* **76**, 1216–1231.

[22] Pocard M, Tsukui H, Salmon RJ, Dutrillaux B, and Poupon MF (1996). Efficiency of orthotopic xenograft models for human colon cancers. *In Vivo* **10**, 463–469.

[23] Siegfried JM, Weissfeld LA, Singh-Kaw P, Weyant RJ, Testa JR, and Landreneau RJ (1997). Association of immunoreactive hepatocyte growth factor with poor survival in resectable non–small cell lung cancer. *Cancer Res* **57**, 433–439.

[24] Zhang YW, Su Y, Lanning N, Gustafson M, Shinomiya N, Zhao P, Cao B, Tsarfaty G, Wang LM, Hay R, et al. (2005). Enhanced growth of human met-expressing xenografts in a new strain of immunocompromised mice transgenic for human hepatocyte growth factor/scatter factor. *Oncogene* **24**, 101–106.

[25] Kankuri E, Cholujova D, Comajova M, Vaheri A, and Bizik J (2005). Induction of hepatocyte growth factor/scatter factor by fibroblast clustering directly promotes tumor cell invasiveness. *Cancer Res* **65**, 9914–9922.

[26] Qian LW, Mizumoto K, Maehara N, Ohuchida K, Inadome N, Saimura M, Nagai E, Matsumoto K, Nakamura T, and Tanaka M (2003). Co-cultivation of pancreatic cancer cells with orthotopic tumor–derived fibroblasts: fibroblasts stimulate tumor cell invasion via HGF secretion whereas cancer cells exert a minor regulative effect on fibroblasts HGF production. *Cancer Lett* **190**, 105–112.

[27] Tsao MS, Zhu H, Giaid A, Viallet J, Nakamura T, and Park M (1993). Hepatocyte growth factor/scatter factor is an autocrine factor for human normal bronchial epithelial and lung carcinoma cells. *Cell Growth Differ* **4**, 571–579.

[28] Yi S and Tsao MS (2000). Activation of hepatocyte growth factor–met autocrine loop enhances tumorigenicity in a human lung adenocarcinoma cell line. *Neoplasia* **2**, 226–234.

[29] To CT and Tsao MS (1998). The roles of hepatocyte growth factor/scatter factor and met receptor in human cancers [review]. *Oncol Rep* **5**, 1013–1024.

[30] Rong S, Jeffers M, Resau JH, Tsarfaty I, Oskarsson M, and Vande Woude GF (1993). Met expression and sarcoma tumorigenicity. *Cancer Res* **53**, 5355–5360.

[31] Rong S, Segal S, Anver M, Resau JH, and Vande Woude GF (1994). Invasiveness and metastasis of NIH 3T3 cells induced by Met–hepatocyte growth factor/scatter factor autocrine stimulation. *Proc Natl Acad Sci USA* **91**, 4731–4735.

[32] Liu J, Blackhall F, Seiden-Long I, Jurisica I, Navab R, Liu N, Radulovich N, Wigle D, Sultan M, Hu J, et al. (2004). Modeling of lung cancer by an orthotopically growing H460SM variant cell line reveals novel candidate genes for systemic metastasis. *Oncogene* **23**, 6316–6324.

[33] Rong S, Bodescot M, Blair D, Dunn J, Nakamura T, Mizuno K, Park M, Chan A, Aaronson S, and Vande Woude GF (1992). Tumorigenicity of the met protooncogene and the gene for hepatocyte growth factor. *Mol Cell Biol* **12**, 5152–5158.

Supplemental Materials and Methods

Gelatin Zymography

Xenograft tumors from inoculating H460 cell line together with H460-pBMN vector control and H460-pBMN harboring Met, HGF, and HGF/Met co-overexpressing cell lines (clones 4-8 and 4-9) were homogenized in lysis buffer (1% Triton X-100, 10% glycerol, 50 mM HEPES, 150 mM NaCl, 1.5 mM $MgCl_2$, 10 mM sodium pyrophosphate, 100 mM NaF, 10 mM $Na_4P_2O_4$, 1 mM EDTA, 10 mg/ml aprotinin, 10 mg/ml leupeptin, 100 mg/ml phenylmethylsulfonyl fluoride, and 1 mM sodium orthovanadate), and the lysates were cleared by centrifugation. The conditioned media from cell lines were collected after 48 hours of serum starvation of the cells. Proteins (30 μg per sample) were diluted in nonreduced SDS sample buffer and separated by electrophoresis in 10% SDS–polyacrylamide gels copolymerized with 1 mg/ml gelatin (for MMP-2 and MMP-9 activity detection). Gels were washed with 2.5% Triton X-100 for 1 hour and then twice in Tris-HCl (pH 8.0) for 15 minutes at room temperature. The gels were incubated with substrate buffer (50 mM Tris-HCl [pH 8.0] and 10 mM $CaCl_2$) for 18 hours at 37°C. The gels were then stained with Coomassie brilliant blue and destained until the clear bands of lysis appeared. To confirm the lytic bands, gels were treated with 20 mM EDTA (a metalloproteinase inhibitor) in the substrate buffer for 18 hours at 37°C.

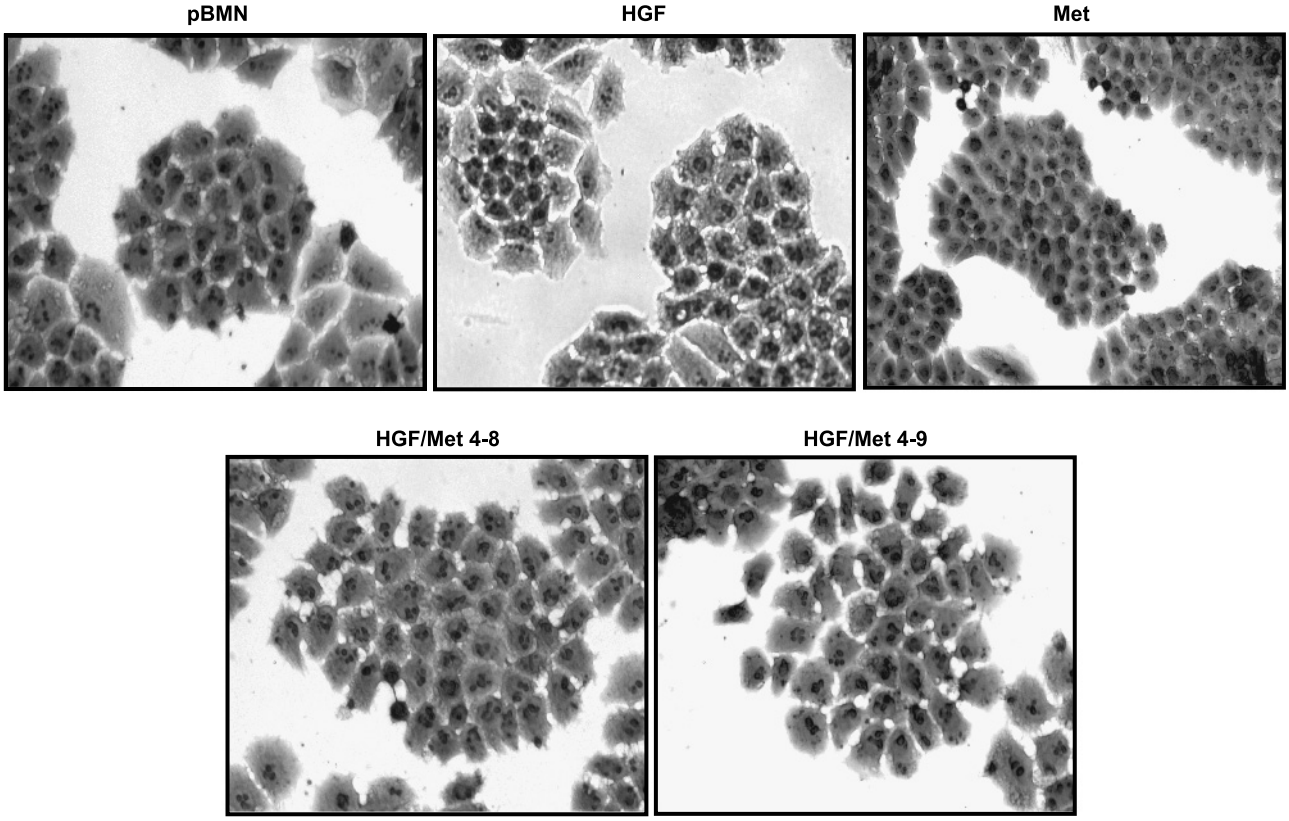

Figure W1. Overexpression of HGF in H460 cell lines had no effect on cell morphology. The morphology of HGF-, Met-, and HGF/Met–overexpressing H460 cell lines were visualized after staining them with crystal violet (0.2%).

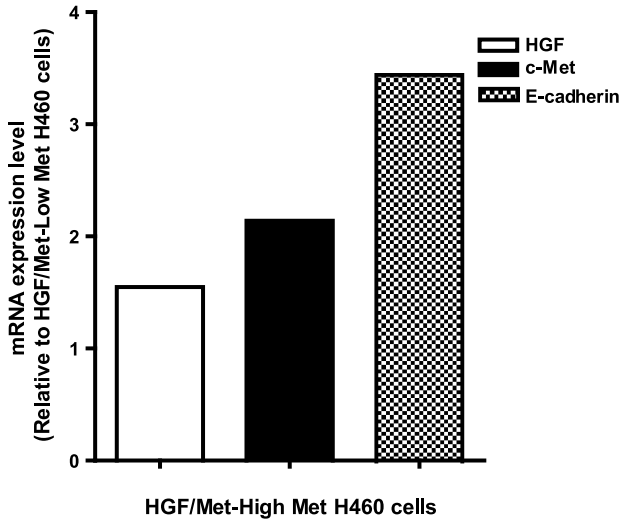

Figure W2. Expression of E-cadherin in high hHGF/Met–expressing cells. The mRNA expressions of hHGF, c-Met, and E-cadherin in HGF/Met 4-9 H460 cell lines with a high expression level of c-Met were evaluated using RT-qPCR and compared with the expression level of the same genes in HGF/Met 4-9 H460 cell lines with a low expression level of c-Met.

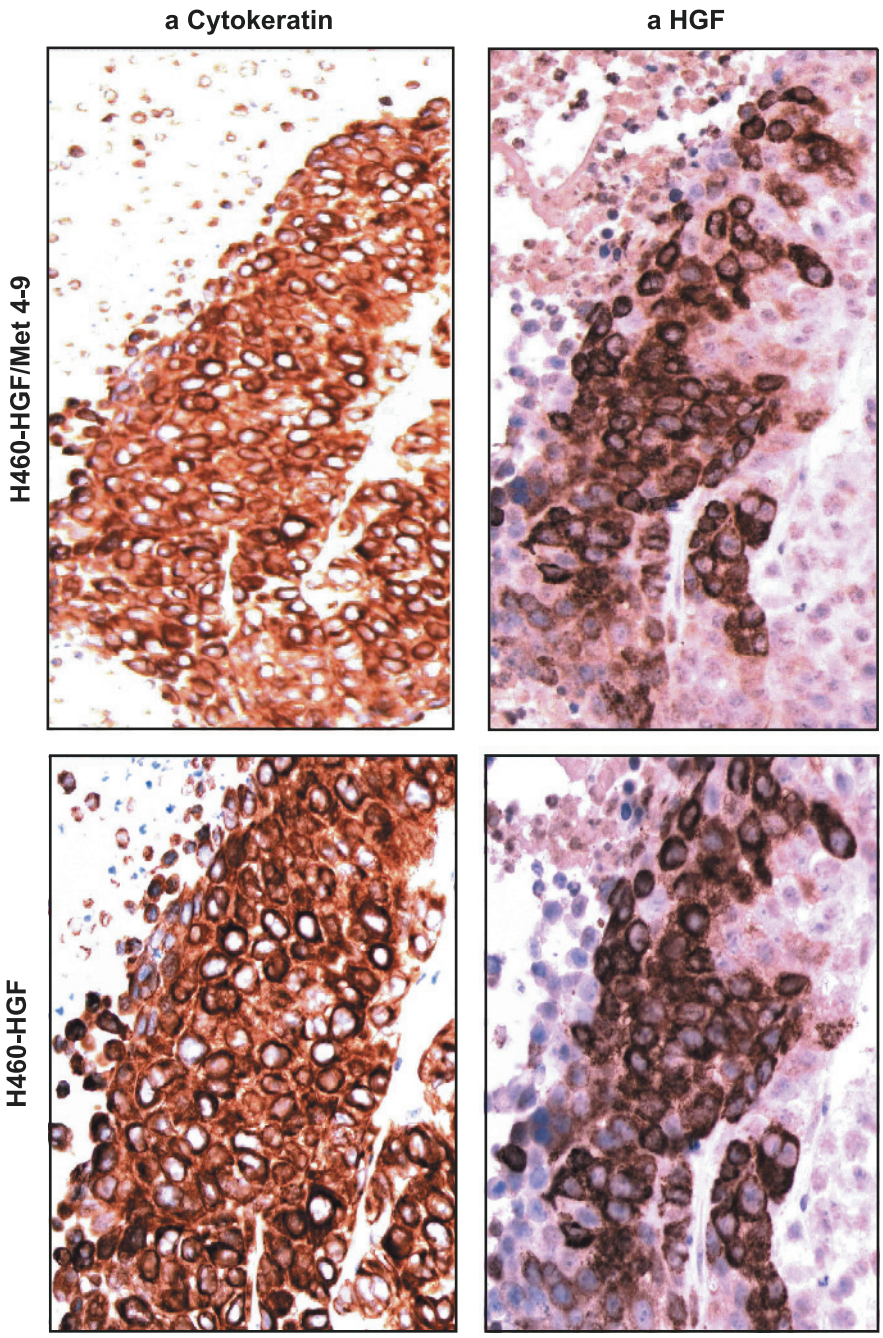

Figure W3. HGF and cytokeratin expression in xenograft tumors appeared to be homogenous, and cells are considered to be epithelial. Xenograft tumors from inoculation of stable HGF- and HGF/Met 4-9–overexpressing H460 cell lines were analyzed by immunohistochemistry for the hHGF (R&D Systems), and human cytokeratin Cam 5.2 (BD Company) specific antibodies at a magnification of ×400.

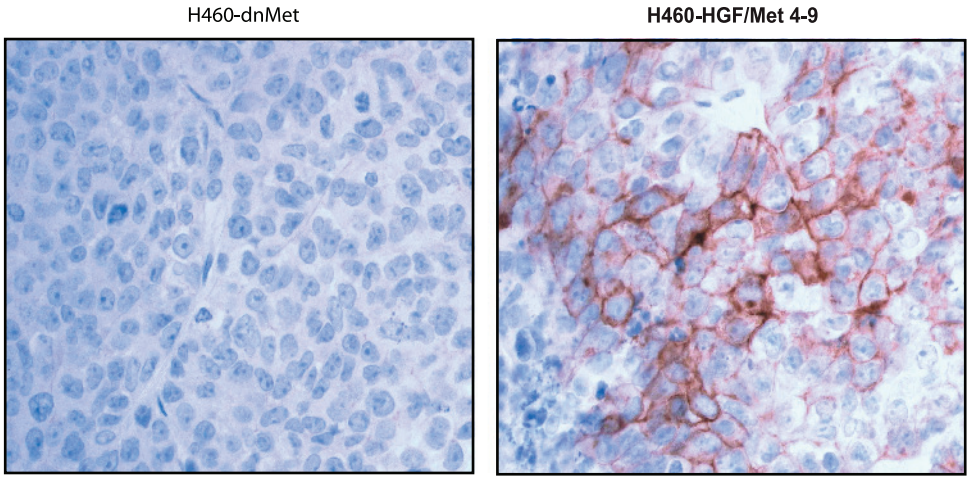

Figure W4. Xenograft tumors from inoculation of stable dnMet and co-overexpressing HGF/Met-H460 (clone 4-9) cell lines were analyzed by immunohistochemistry for the activated receptor using phospho-Met–specific antibody (pMet) at a magnification of ×400.

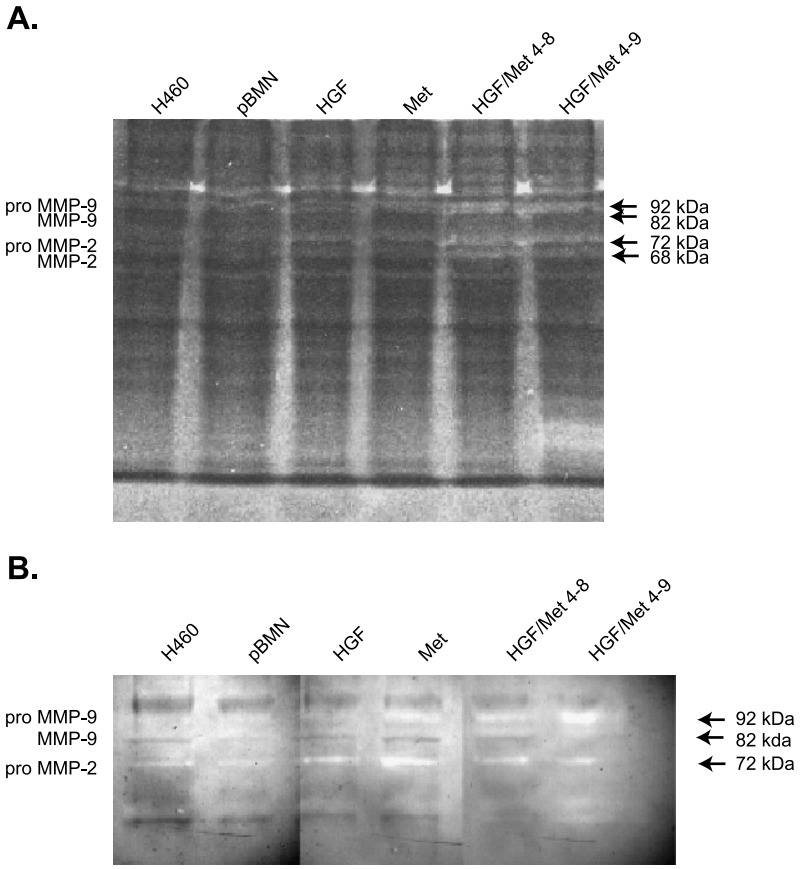

Figure W5. Enhanced activity of MMP-9 and MMP-2 in HGF/Met–overexpressing H460 cell lines. (A and B) Using gelatin zymography in both *in vitro* (A) and *in vivo* (B), we demonstrated higher levels of both proactive and active form of MMP-9 (92 and 82 kDa, respectively) and MMP-2 (72 and 68 kDa, respectively) when both HGF and c-Met were overexpressed compared with pBMN control and parent H460. The bands show the lytic zones.